



**Micelle Stability in Water under Pressure and Temperature;  
Have both a Common Mechanism?**

Journal:	<i>RSC Advances</i>
Manuscript ID:	RA-ART-05-2015-009377.R2
Article Type:	Paper
Date Submitted by the Author:	25-Jul-2015
Complete List of Authors:	Grigera, J. Raúl; CEQUINOR, Espinoza Silva, Ricardo; CEQUINOR, ; CEQUINOR,



## Micelle Stability in Water under Pressure and Temperature; Have both a Common Mechanism?

Received 00th January 20xx,  
Accepted 00th January 20xx

DOI: 10.1039/x0xx00000x

www.rsc.org/

Yanis Ricardo Espinosa Silva<sup>a</sup> and J. Raul Grigera<sup>a, †</sup>

The formation of sodium dodecylsulfate (SDS) micelles in water and heavy water at different pressures and temperatures using Molecular Dynamics simulations was used to analyze their stability and structure under different conditions and to evaluate the agreement between existent experiments. The results reproduced the assembling of micelles at 1 bar and the presence of larger aggregates under high pressure (over 3 kbar). These large aggregates are not micelles but small finite pieces of bilayers in rod-like. The results obtained on systems at different temperatures showed that both high and low temperatures produce lamellar structures. It is well known that micelles expose polar residues to water and leave non-polar residues inside where they interact by hydrophobic interactions. High pressure and low and high temperatures inhibit hydrophobic interaction, and under these conditions, other structures are produced instead of micelles. This process seems to be similar to protein denaturation under temperature and pressure.

### Introduction

The stability of aggregates of amphiphilic surfactants in water under pressure and temperature has been widely discussed in the literature.<sup>1-10</sup> Results obtained with various experimental techniques (conductivity, light scattering, dynamic fluorescence probe, and small-angle neutron scattering) indicate that micelles are formed in an aqueous solution of surfactants at 1 bar when sodium dodecylsulfate (SDS) (See figure 1) concentration reaches the critical micelle concentration (CMC). Increasing pressure, the aggregation number decreases and, around 1 kbar, micelles are disassembled. At higher pressure large aggregates appear which was interpreted as a re-entrance of the micellar phase with larger aggregate numbers. It is widely accepted that hydrophobic interaction is the driving force for the assembling of micelles, but we have to be aware that at a pressures above 1 kbar, water changes its structure decreasing the ratio Low/High water structure the hydrogen bond lattice weakening, or even eliminating, the hydrophobic interactions. This fact seems to contradict the possibility of large micelles at high pressures. Recently, Baltasaret.*al.*<sup>6</sup> have using sound speed technique on sodium dodecanoate water solution under pressure suggesting that a gel-like phase is formed above 2.5 kbar. We cannot ignore the experimental evidence of the existence of large aggregates at high pressure. Thus, with the aim of contributing to the explanation of the apparent discrepancy on the nature of the properties of water surfactant mix under pressure we studied the behaviour of a solution of SDS in water and heavy water at different pressures and temperatures using Molecular Dynamics Simulation.

### Computational methods

The systems under study were a mixture of sodium dodecylsulphate in water or heavy water. The model of SDS used was developed by Sammalkorpi and co-workers<sup>7</sup> (See figure 1). For water, we used the Simple Point Charge Extended model (SPC/E)<sup>11</sup> and for heavy water the Simple Point Charge Heavy Water (SPC/HW).<sup>12</sup> Molecular Dynamics (MD) simulations were done using the GROMACS 4.5.3 package,<sup>13</sup> the equations of motion were solved using a leap-frog integration step. We used a cubic simulation box, with periodic boundary condition. The systems were initially equilibrated with the NPT ensemble at 300 K and 1 bar and then fixing the required temperature and pressure were then fixed using a weak coupling with V-rescale thermostat<sup>14</sup> and Berendsen barostat<sup>15</sup> with coupling time constants of 0.1 ps and 1.0 ps, respectively. The Lennard-Jones (LJ) interactions and long-range electrostatic interactions were cutoff at 1.2 nm, to calculate long-range electrostatic interactions we use the Reaction Field method.<sup>16</sup> Throughout the simulations the integration time step was 2 fs. Water molecules and SDS were constrained using the LINCS algorithm.<sup>17</sup>

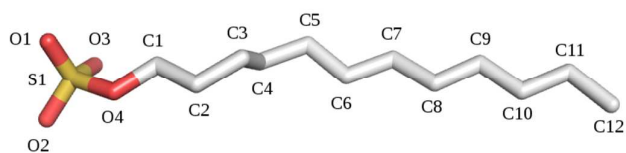


**Figure 1.** Sodium dodecylsulfate molecule employed in our MD simulations with the reference numbers of each atom.

<sup>a</sup> CEQUINOR, University of La Plata and CONICET. 47 y 115, B1900. La Plata, Argentina.

<sup>†</sup> e-mail, raul@grigera.com.ar



## ARTICLE

## Systems under pressure

The simulations started with a random distribution of SDS/water mixture at a concentration above the CMC. We first study the behaviour of self-aggregation of SDS in SPC/E and SPC/HW varying the SDS numbers and water molecules at constant concentration (500 mM). Thus, 70 and 200 SDS molecules were hydrated with 6667 and 16792 solvent molecules, respectively. The configurations that resulted after the self-aggregation process were used as starting points of simulations under pressure. After equilibrium at 1 bar, the system was coupling to barostat increasing the pressure at regular steps up to 4000 bar.

For each selected pressure, the systems of 70 and 200 SDS were simulated during 10 ns and 100 ns, respectively. The data was collected after equilibration during 5 ns and 50ns, respectively.

## Cluster analysis

Cluster analysis was done using Stillinger's direct connectivity criterion,<sup>18</sup> where the connecting time is not required, checking connectivity for each frame, *i.e.*, this criterion is based solely upon the distance between particles. Therefore, two molecules are considered members of a cluster when the distance between the C6-carbon atoms is less or equal to 3/2 of the diameter ( $\sigma$ ) ( $R_{\text{cut}} = 0.60\text{nm}$ ). The molecules were selected using the algorithm of Stoodart.<sup>19</sup>

We can define probability  $P_s$  to find a cluster of  $s$  monomers as<sup>20</sup>:

$$P_s = \frac{n(s)s}{N}, \quad (1)$$

Where  $n(s)$  is the number aggregates of  $s$  monomers and  $N$  is the total number of monomers. The ratio  $n(s)/N$  can be considered as a relative frequency, thus  $P_s$  satisfies the normalization condition.

$$\sum_{s=1}^N P_s = 1 \quad (2)$$

The aggregation process can also be analyzed using the radial distribution function,  $g(r)$ . For all pairs of SDS molecules, we plotted the first peak of the radial distribution function between the C1 and C12 carbon atoms against pressure. The SDS solvent accessed surface was calculated using the `g_sas` algorithm<sup>13</sup> with a probe radius of 1.4 Å.

## Results and discussions

## Self assembly

As we stated before, the criteria adopted to define the formation of micelles was based on a geometrical classification of the distance between the C6-atoms of all SDS molecules. The solutions at the desired concentration (500 mM) were randomly distributed in a simulation box of arbitrary size and the simulation was started at 1 bar and 300 K. After equilibration, a longer run was carried out to collect enough data. Figure 2 shows the normalized cluster size against the aggregation number along 100 ns of simulation after equilibration.

The aggregation process over time was monitored recording the area of SDS exposed to the solvent. Figure 3 corresponds to a system of 200 SDS monomers and 16972 SPC/E water or SPC/HW heavy water, respectively (500mM for both systems) at 300K and 1 bar. We can see that the micelles were formed around first 20 ns. For D<sub>2</sub>O, the final exposed area was lower than for H<sub>2</sub>O. This difference was in agreement with the slightly stronger energy of the D-bond compared with the H-bond.

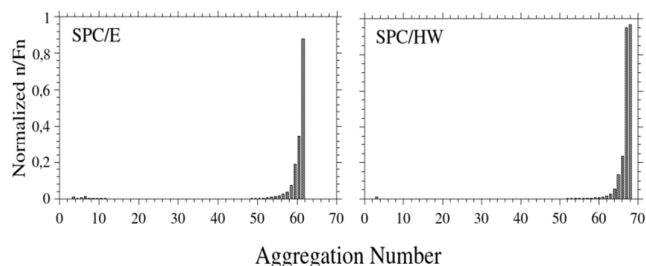


**Figure 2.** Maximum aggregation number in the micellization in a system with 70 SDS molecules. Normalized distribution function of cluster against aggregation number of SDS in water (SPC/E) and heavy water (SPC/HW) at 500 mM.

The maximum aggregation number in the system of 70 molecules in SPC/E was 62 SDS molecules. For SPC/HW, at the same concentration, the formed micelles had a size of between 65 to 67 monomers. It should be noted that the temperature was set slightly higher than the critical micellization temperature (CMT) reported for SDS.<sup>21</sup>

To test whether the results depend on the system size, we have built a system 200 monomers at 500 mM. The results showed that were not significant differences in micellization (See fig. S1 and S2, in supplementary information).



## ARTICLE

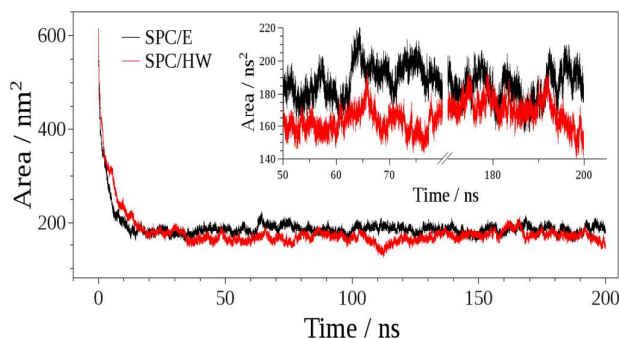


**Figure 3.** Changes over time of the SDS exposed to the solvent in water (black) and heavy water (red). Inset show zoom of the area of SDS exposed to the solvent.

#### Micelles under pressure

We studied the effects of pressure on the micelles already formed by analyzing the phase transition between the states at 1 bar and 4000 bar at  $T = 300$  K. The structures were evaluated by plotting the first peak of the radial distribution function of the carbon atoms ( $C_1$ - $C_{12}$ ) (See figure 1)) against pressure.

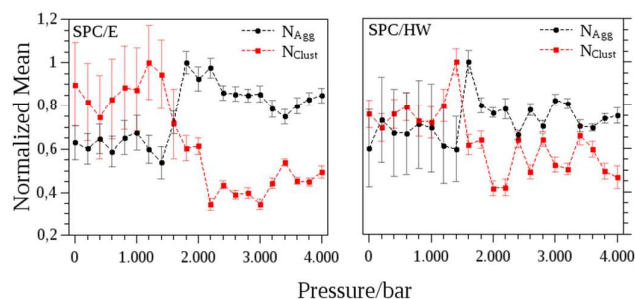
To describe the structural changes of micelles at different pressures, we computed the average number of clusters ( $N_{\text{clust}}$ ) and the average aggregation number ( $N_{\text{agg}}$ ) for a range of pressure between 1 bar and 4 kbar in a system of 70 SDS and 200 SDS monomers. A version with solvent was SPC/E water and SPC/HW heavy water was simulated for each of those systems.

Figure 4 shows the changes in  $N_{\text{agg}}$  and  $N_{\text{clust}}$  at different pressures to a system of 70 SDS monomers. We can observe that in water, the average aggregation number  $N_{\text{agg}}$  (black lines) started to decrease at around 1 kbar and reached a minimum at around 1400 bar. From that point, a sharp increase was observed, reaching a large aggregation number. Accordingly, the number of clusters  $N_{\text{clust}}$  followed the opposite trend (red lines), close to 1200 bar  $N_{\text{clust}}$  display the maximum value, starting to diminish until 2200 bar. In heavy water, we observed that although demicellization kinetic seems to have the same trend as water, in SPE/HW the most energy on the D-bond makes more difficult the micellar disassembled and the formation of smaller aggregates.

This behaviour was experimentally observed by light scattering<sup>1</sup> and interpreted as a partial disassembling around 1 kbar, with the formation of a larger number of micelles of smaller size and, at larger pressure, a decrease in the number the micelles accompanied by an increase in size.

The present results were consistent with the experiments, since at 1 bar we observed a number of aggregates (micelles) which, when pressure increased, were segregated at least partially, (large

number of small clusters). At pressures above but close to 1 kbar, we found a lower number of larger aggregates. When pressure increased, larger lamellar-like aggregates were produced. We have to bear in mind that the number of clusters computed with this method includes elements of quite different size. However, we cannot conclude that we are in presence of large micelles at high pressure.



**Figure 4.** Normalized cluster size ( $N_{\text{clust}}$ , red) and Normalized aggregation number ( $N_{\text{agg}}$ , black) for water (SPC/E) and heavy water (SPC/HW). Dots and error bars represent the average and the standard error, respectively

Figure 5 shows a visualization of the process of the changes in the aggregation under pressure following the radial distribution function,  $g(r)$ , normalized for  $C_1$ - $C_{12}$  (see sec Cluster Analysis) in water and heavy water with 200 SDS molecules. This alternative representation also shows that the micellar phase was stable at 1 bar, but the increase of pressure generated a transformation process that, above 2 kbar, led to larger aggregates.

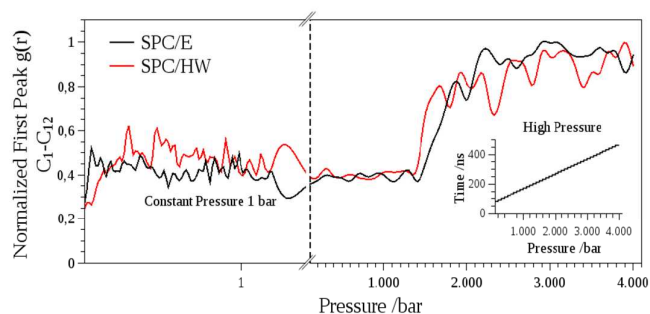


**Figure 5.** Normalized first peak of the radial distribution function of SDS water and heavy water system along the simulation run at different pressures. This representation is consistent with the results of the number of aggregates at different pressure. Normalization was performed by the ratio  $g(r)_0/g(r)_{\text{max}}$ , where  $g(r)_0$  is most probable distance between neighbours atoms and  $g(r)_{\text{max}}$  maximum probability distance the neighbouring atom. (Non-standardized data in Fig. S3 of supplementary information)



## ARTICLE

Figure 6 shows another way of depicting the process by plotting the area of SDS exposed to the solvent. At the bottom of the figure we can see images taken from the simulation that show the behaviour of the aggregation of SDS at three different pressures: at 1 bar micelles; at 1500 bar, partially disassembled aggregates; and at 4000 bar, lamellar structure. It is known that at 1 bar amphiphilic surfactants, such as SDS, which have well defined polar head and hydrophobic tails, tend to form spherical micelles, the polar head interacting with the counter ions of the solution and the hydrophobic tails oriented towards the centre, forming sphere-like micelles.

When pressure increased to 1500 bar, the water began to lose its tetrahedral structure, weakening the hydrophobic interaction;<sup>22-23</sup> the internal micellar core was thus at least partially exposed to the solvent, causing a disassembling of micelles. With a further increase of pressure (4000 bar), large structures were observed that were interpreted as micelles of larger dimensions than the observed at 1 bar.<sup>1</sup>

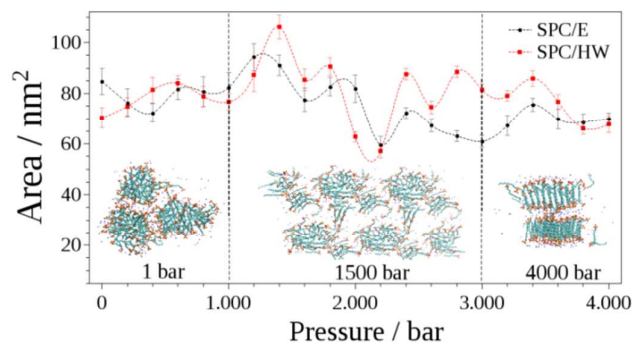


**Figure 6.** Exposed area of 200 SDS monomers in water (black line) and heavy water (red line) at different pressure. The images of aggregates were obtained from the simulation. Dots and error bars represent the average and the standard deviation, respectively.

At a first glance, the image seems to be a lamellar structure; however, as can be observed in Figure 7, which shows the picture corresponding to 4000 bar from two different views, seems to indicate that the lamellar phase actually consists not with extended stacked bilayers but rather of layers of small finite pieces of bilayers (e.g., disks and ribbons)<sup>24</sup>. In our simulations we see that the change in the geometrical aggregation is consistent with a *stacked disk rod* in lamellar phase. This result agrees with Chen and Ruckenstein<sup>25</sup>, who report about effect of the selectivity of the solvent in changing morphologies copolymers aggregation, using dissipative particle dynamics (DPD) simulation. Likewise, Baltasar *et al.*,<sup>6</sup> in an experimental study, noted that the changes in the surfactants aggregation state can be explained in terms of pressure effect on the characteristics of the hydrogen bonding network of water favoring appearance of lamellae phases.

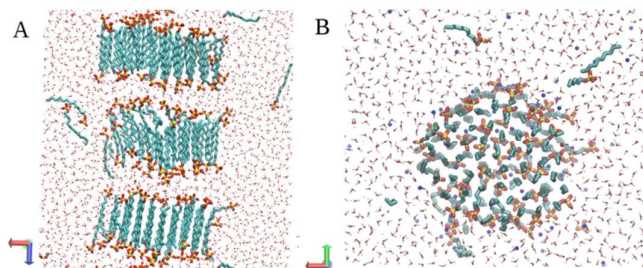


**Figure 7.** Structure of aggregates at 4000 bar. Picture A suggest small finite pieces stacked of lamellar structure. However, considering also picture B (rotated 90 degrees from A) a disk is evident and that structure is a stacked disk rod. The system in this example is observed with 200 SDS molecules, but the change in structure is the same in both systems.

### Temperature effects

The contribution to the free energy of the hydrophobic interaction has entropic origin; therefore, if the temperature decreases, the contribution of the entropic term,  $-\Delta S$ , will decrease too. Thus, we expected that lowering the temperature of a system of SDS in water would have a similar effect than increasing the pressure. On the other hand, high temperature increases the entropy of the system but the aggregation of non-polar regions will not produce additional entropy (the driving force of hydrophobic interactions); as a consequence, we expected aggregates based mainly on polar interactions. To check the hypothesis, we performed a molecular dynamic simulation of a system of SDS in SPC/E water already stabilize at different temperatures. Figure 8 shows the change in the structure of a system already equilibrated at 1 bar at temperatures from 253 to 700 K.

At the low temperature analyzed (253 K), we observed an aggregate that seemed to evolve to a stacked disk rod structure too. The effect of low temperature seemed to be similar to the pressure effect. The image at 273 K shows an intermediate state. At 300 K, we observed regular micelle formation. When temperature increased to 363 K, the structure changed, showing a large aggregate composed of two similar large interacting aggregates but more disordered than the one observed for 253 K, when the formation of stacked disk rod lamellas was in progress. An inverse micelle was observed at 700 K. This structure was due to the fact that at such high temperature water was in vapour phase and the polar interaction produced an inverse micelle shape.



## RSC Advances

## ARTICLE

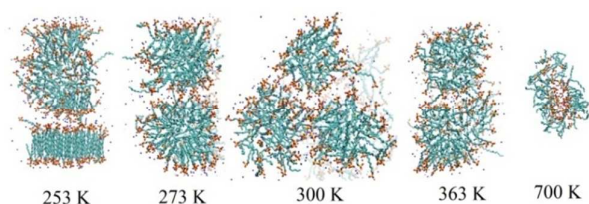


**Figure 8.** Structure of 200 SDS molecules in water at five different temperatures.

### Conclusions

The results obtained by simulation showed that SDS micelles in water were disassembled when pressure increased up to 1 kbar. At higher pressure, a rearrangement process was observed, producing stacked disk rod structures. The changes at high pressure can be explained by considering the changes in water under pressure from a predominantly hexagonal structure, Low-density (LD) to a predominantly tetrahedral one-High-density (HD). These structural changes result in a process of gradual inhibition of the hydrophobic interaction when pressure increases. Micelles are formed in SDS at normal pressure due to the association of non-polar tail, exposing the polar head to the solvent neutralized by the counter-ions. At around 1 kbar, the hydrophobic interaction was weaker, allowing the exposure of the non-polar tails. With a further increase of pressure, the system was compacted. Non-polar tails can associate by weak attraction, exposing their surface to the solute without restriction. At the same time, polar heads associate with each other with the help of counter-ions, producing a compact structure with lamellar shape. It was experimentally shown that large aggregates are formed at high pressures, which are compatible with the stacked disk rod shape shown by the simulation results.

Regarding the temperature effect, we observed that both low and high temperatures produced similar structures than high pressure. This is understood since the hydrophobic interaction depends on the entropic contribution of the free energy ( $-T\Delta S$ ). Therefore, at high temperature and a low temperature, the association of non-polar solutes will not increase entropy through the association of non-polar residues, producing different structures. This process is similar to the temperature and pressure denaturation of proteins<sup>26</sup>. Due to the similitude of the changes on both systems, we might name the phenomenon of the micelle structure at low temperature and high pressure as *micelle denaturation*.

### Acknowledgements.

We wish to thank to Dr Ernesto Caffarena for your interesting comments and to Dr. Ariel Alvarez for his help with MD simulations.

The work was funded by the National Council of Argentina (CONICET) and the University of La Plata (UNLP); Y.R. Espinosa was supported by the CONICET and J.R. Grigera is member of the Research Carrere of same institution and Emertius Professor of the UNLP.

### References

- 1 N. Nishikido, M. Shinozaki, G. Sugihara, M. Tanaka and S. Kaneshina, *Journal of Colloid and Interface Science*. 1980, **74**, 474.
- 2 K. Hara, N. Baden and O. Kajimoto, *J. Phys. Condens. Mater.* 2004, **16**, S1207.
- 3 J. S. Collura, D.E. Harrison, C.J. Richards, T.K. Kole, and M.R. Fisch, *Langmuir* 2001, **17**, 8084.
- 4 R. De Lisi, S. Milioto and N. Muratore, *J. Phys. Chem. B*. 2001, **105**, 4846.
- 5 S. Kaneshina, M. Tanaka, T. Tomida and R. Matuura, *J. Coll. Int. Sc.* 1974, **48**, 450.
- 6 E.H. Baltasar, M. Taravillo, P. Sanz, D. Baonz and B. Guignon, *Langmuir*, 2014, **30**, 14743-47477.
- 7 M. Sammalkorpi, M. Karttunen and M. Haataja, *J. Phys. Chem. B.*, 2007, **111**, 11722-11733.
- 8 K. Hara, H. Suzuki and N. Takisawa, *Phys. Chem.* 1989, **93**, 3710-3713.
- 9 A. Jusufi, S. A. Sanders, M. L. Klein, and A. Z. Panagiotopoulos, *J. Phys. Chem. B*, 2011, **115**, 990-1001.
- 10 S. A. Sanders, M. Sammalkorpi, and A. Z. Panagiotopoulos, *A. Z. J. Phys. Chem. B*, 2012, **116**, 2430-2437.
- 11 H. J. C. Berendsen, J.R. Grigera and T.P. Straatsma, *J. Phys. Chem.* 1987, **91**, 6269-6271.
- 12 J.R. Grigera, *J. Chem. Phys.* 2001, **114**, 8064-8067.



## RSC Advances

## ARTICLE

- 13 D. Van Der Spoel, E. Lindahl, B. Hess, G. Groenhof, A.E. Mark and H.J. Berendsen, *J. Comput. Chem.* 2005, **26**, 1701-1718.
- 14 G. Bussi, D. Donadio, and M. Parrinello, *J. Chem. Phys.* 2007, **126**, 014101-014107.
- 15 H.J. Berendsen, J.P.M. Postma, W.F. vanGunsteren, A.R.H. DiNola and J.R. Haak, *J. Phys. Chem.*, 1984, **81**, 3684-3690.
- 16 I.G. Tironi, R. Sperb, P.E Smith and W.F.A vanGunsteren, *J. Chem. Phys.* 1995, **102**, 5451-5459.
- 17 B. Hess, H. Bekker, H.J. Berendsen, and J.G Fraaije, *J. Comp.Chem.* 1997,**18**, 1463-1472.
- 18 F.H. Stillinger, *J. Chem. Phys.* 1963, **38**, 1486-1494.
- 19 S.D. Stoddard, *J. Comput. Phys.* 1978, **27**, 291-293.
- 20 D. Stauffer and A. Aharony, in *Introduction to Percolation Theory*, Taylor & Francis, London, 2nd edn., 1994, pp. 15-60.
- 21 S. Paula, W. Sues, J. Tuchtenhagen and A. Blume, *J. Phys. Chem.* 1995, **99**, 11742-11751.
- 22 O. Chara, A.N. McCarthy, and J.R. Grigera, *Phys.Lett. A.* 2011, **375**, 572-576.
- 23 C.G. Ferrara and J.R. Grigera, *Chemical Physics.* 2014, **434**, 15-19.
- 24 W.M. Gelbart, and A. Ben-Shaul, *J. Phys. Chem.* 1996, **100**, 13169-13189.
- 25 (a) H. Chen, and E. Ruckenstein, *Soft Matter*, 2012,**8**, 8911-8916; (b) H. Chen, and E. Ruckenstein, *Soft Matter*, 2012,**8**, 1327-1333.
- 26 C.L. Dias, T. Ala-Nissila, J. Wong-ekkabut, I. Vattulainen, M. Grant and M. Karttunen, *Cryobiology.*2010, **60**, 91-99.